On the determination of the poloidal velocity and the shear layer in the SOL of ASDEX Upgrade

F. Mehlmann[1], S. Costea[1], V. Naulin[2], J.J. Rasmussen[2], H.W. Müller[3], A.H. Nielsen[2], N. Vianello[4], D. Carralero[3], V. Rohde[3], C. Lux[1], R. Schrittwieser[1], C. Ionita[1], ASDEX Upgrade Team[3]

[1]*Inst. Ion Phys. &. Appl. Phys. , EURATOM-ÖAW Association, University Innsbruck, Austria*
[2]*Association EURATOM/DTU, Dept. of Physics, DTU Risø Campus, Roskilde, Denmark*
[3]*Max-Planck-Institute for Plasma Physics, EURATOM Association, Garching, Germany*
[4]*Consorzio RFX, Associazione Euratom-ENEA sulla Fusione, Padova, Italy*

Abstract: A reciprocating probe with six pins was used for localized measurements in the scrape-off layer (SOL) of ASDEX Upgrade (AUG) up to the shear layer (SL) and a few mm inside it. The probe was used to determine the poloidal velocity with three different methods which are critically compared to each other concerning their reliability. Furthermore, we have determined the position of the shear layer.

1. Introduction

Fig. 1 shows the front side of the "Innsbruck-Padua" probe head [1] and the biasing scheme of the pins. There are six graphite probe pins of 1 mm diameter and 2 mm length. One pin (#6) protrudes by 3 mm , thus being further inside. The difference between the floating potentials of pins #6 and #8, divided by their radial separation of $d_{6,8}$ = 3 mm, yields an approximation of the radial electric field $E_r = (V_{fl,6} - V_{fl,8})/d_{6,8}$ from which the poloidal velocity v_p is derived.

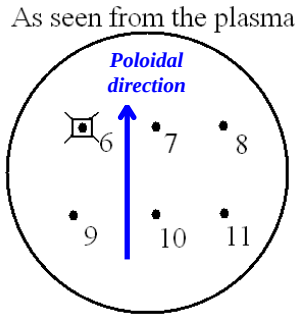

Fig. 1: Front side of the "Innsbruck-Padua" probe head (50 mm diameter, 115 mm length) with six probe pins of 1 mm diameter and a length of 2 mm each: pin #6 (3 mm protruding radially) – floating,# 7 – biased for I_{sat}, #8 – floating, #9 – swept, #10 – I_{sat}, #11 – floating. The toroidal/ poloidal distances between the pins are 10 mm.

The toroidal distance of 20 mm between pins #6 and #8 does not matter since the toroidal electric field can be neglected on this distance. Obviously we had to assume that the electron temperature T_e is equal on both pin positions. However, we measure partly in a region with a steep gradient of T_e. But in absence of a diagnostic tool measuring the plasma potential directly whence all relevant electric field components can be derived, and/or a reliable diagnostic for T_e with sufficient temporal resolution to resolve also T_e fluctuations, we had to be content with the present opportunity. In addition the cross correlation (CC) was determined of the ion saturation currents $I_{sat7,10}$ of probe pins #7 and #10 and of the floating potentials $V_{fl8,11}$, measured by pins #8 and #11.

2. Experimental method

In the following, exemplary results of AUG shot #28877 are shown, during which four probe strokes were executed. The insertion and retraction velocity of the probe head were adjusted

such that the radial profiles of the parameters could be determined with sufficient resolution with respect to the radius r, for which the reference point ($r = 0$) was the limiter of the ICRH antenna. The results shown below have been taken during probe retraction during the fourth probe stroke.

The global parameters of L-mode shot #28877 are given in the following table.

Main parameters	I_{pl} (MA)	n_e (m^{-3})	B_t (T)	P_{ECRH} (MW)	q_{95}	*Flat top time*
L-mode #28877	1,00	$4{,}4 \cdot 10^{19}$	–2,43	0,484, (1,500 – 5,091 s)	4,105	1,120 – 5,258 s

I_{pl} is the plasma current, n_e the electron density, B_t the toroidal magnetic field, P_{ECRH} the power of electron cyclotron resonant heating, and q_{95} is the safety factor at 95% of normalized poloidal flux.

To derive the poloidal velocity v_p three methods have been used:

1) By assuming it as being due solely to the $\boldsymbol{E}\times\boldsymbol{B}$ drift and using $E_r = (V_{fl,6} - V_{fl,8})/d_{6,8}$, while B_t is known (see Fig. 2): $v_p = E_r/B_t$
2) From the CC of the signals of the two ion-biased probe pins #7 and #10, which deliver the time lag for maximum CC, choosing time windows of appropriate lengths. Thence for each time, respectively radial probe position, we obtain: $v_p = d_{7,10}/t_{lag,sat}$.
3) Similarly from the CC of the signals of the floating probe pins #8 and #11,: $v_p = d_{8,11}/t_{lag,fl}$.

3. Experimental results and discussion

Fig. 2 shows the radial profile of the poloidal velocity $v_p = E_r/B_t$, determined by method 1, from the above list. The red symbols show the data after smoothing, since the spread of the original data is very strong [2]. The reference position of the probe head ($r = 0$) is the ICRH limiter with the radial position decreasing to the left, i.e. higher negative values mean the probe is deeper in the SOL. The shown data have been taken during the retraction of the probe. We see that $v_p(r)$, starting from a value around zero, becomes very negative rather abruptly at $r \cong -40$ mm reaching maximum values of around –3000 m/s. This sudden change of the poloidal velocity occurs in the shear layer (SL), so that we take the approximate position of the steepest gradient of the increase of v_p as an indication of the SL, i.e. the $r_{sl} \cong -43$ mm. This is indicated in the diagram by a vertical red bar.

Fig. 3(a,b) shows the results of methods 2 and 3, i.e. determining the poloidal velocity from the CC of the I_{sat} signals (Fig. 3(a)) and the V_{fl} signals (Fig. 3(b)). In this case we show the time lags of the CC instead of the actual velocities. To observe the differences better, the two methods are compared in terms of the time t of the motion of the probe head rather than its actual radial position r. In Fig. 3(a) also the "time lag" corresponding to v_p, determined by method 1, is shown by a black line. Also in these graphs going from left to right on the time axis t corresponds to the retraction of the probe during stroke 4.

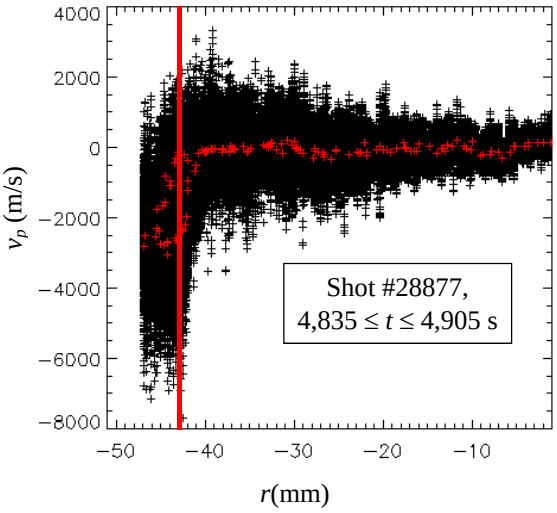

Fig. 2: Radial profile of the poloidal velocity v_p, deduced through $\boldsymbol{E}_r \times \boldsymbol{B}_t / B_t^2$. E_r was determined from the difference of the floating potentials of two cold probes separated radially by 3 mm. The red symbols show the smoothed values. The vertical red bars indicate the approximate position of the shear layer as determined by the methods described in the text. The zero point of the radial scale is the position of the ICRH limiter (shot #28877).

Just like the sudden change of v_p in Fig. 2, also the time lags corresponding to maximum correlation in Figs. 3(a) and (b) should show sudden jumps in the SL. In both figures in the top panels the red horizontal bar shows, for comparison, the position of the SL as determined from Fig. 2 at $r_{sl} \cong -43$ mm. On the time scale this corresponds to a time position of the probe of $t \cong 4{,}850$ s. In both figures, the vertical red lines show this position on the time scale of the probe motion.

Indeed near this time also the time lag of the CC maxima shows sudden jumps. In Fig. 3(a), showing the CC of the saturation currents, the time lag changes somewhat further outside, i.e. for $t \cong 4{,}852$ s. For $t < 4{,}852$ s the time lag of maximum CC, shown by the green range, is very small, actually slightly positive. For $t > 4{,}852$ s it drops to negative values of $t_{lag,sat} \cong -7$ μs (the dark blue line indicates this jump). This corresponds to a poloidal velocity of around –1430 m/s. Expectedly the black line, showing the time lag corresponding to v_p as determined by method 1 ($E_r \times B_t$-drift), also shows a drop to similar values as $t_{lag,sat}$.

Fig. 3(b), showing the CC of the floating potentials, the conditions are more complicated, since there are two jumps (also demonstrated by a dark blue line) of the time lags of the CC maxima: for $t > 4{,}845$ s the maxima jump from a positive value $t_{lag,fl} \cong 3{,}5$ μs to a value slightly above zero. For $t > 4{,}856$ s a jump to negative values $t_{lag,fl} \cong -6$ μs occurs. This corresponds to a poloidal velocity of around –1670 m/s.

4. Discussion and Conclusion

With respect to the qualitative behaviour the three methods yield similar results, in particular concerning the SL, where for methods 2 and 3 (CC of the I_{sat}-signals – Fig. 3(a) and of the V_{fl}-signals – Fig. 3(b)) jumps of the time lag occur and also v_p determined through method 1 (the $E_r \times B_t$-drift) suddenly decreases strongly (Fig. 2). Thus the SL occurs somewhere around $t > 4{,}85$ s, corresponding to a value of $r \cong -43$ mm. However, the double jump in Fig. 3(b) is hardly explicable. On the other hand the values of the poloidal velocity outside the SL (at least roughly for $t > 4{,}856$ s) agree rather well: they are in the range of –1500 m/s for methods 2 and 3. In contrast to that, method 1 delivers a much smaller value for v_p for $r > -40$ mm.

Inside the SL we obtain much stronger discrepancies between the results of all three methods: method 1 shows a small negative value of the time lag for $t < 4{,}85$ s, method 2

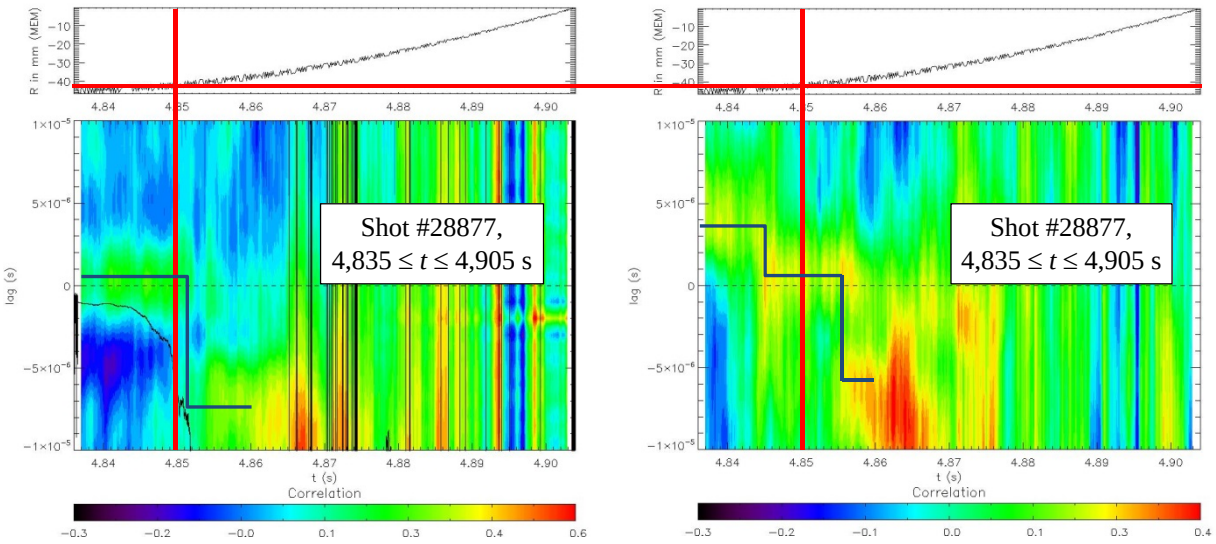

Fig. 3: Top graphs show relative positions r of the probe head from the ICRH limiter versus time of probe position. Bottom graphs show time lags of cross correlation (a) of the two I_{sat}-probes #7 and #10 (the black line shows the time lag determined through v_p (see Fig. 2) by method 1, i.e. the $\boldsymbol{E}_r \times \boldsymbol{B}_t$-drift), (b) of the two floating probes #8 and #11. The colour scales show the intensity of the CC. Approximate position of the SL, taken from Fig. 2, at $r \cong -43$ mm and $t \cong 4{,}85$ s is indicated by the horizontal red bar in the top graphs and by the vertical red bars in both graphs. The dark blue lines indicate the jumps of the time lags discussed below.

seems to indicate a slightly positive value although the green range is broad covering also values below zero. Method 3 shows for $t < 4{,}845$ s a definitely positive value.

It is plausible that these discrepancies are mostly due to the fact that in lack of a better diagnostic (as discussed above) we measure here with cold probes so that the electron temperature has a great influence on the determination especially of the electric field components [2]. This would also make it plausible why stronger discrepancies are found inside the shear layer where T_e is much higher having an especially strong gradient through the SL.

We would like to emphasize also that in other probe strokes both CC methods sometimes showed jumps also far outside the SL, i.e. in the range $r > -30$ mm.

Our results again show that for reliable localized measurements of electric fields in the SOL and in particular further inside, improved plasma probes such as ball-pen probes or permanently heated emissive probes are a necessity, which can measure at least the radial and poloidal electric field components.

Acknowledgements

This work, supported by the European Communities under the Contracts of Associations between EURATOM and ÖAW, IPP, ENEA-RFX and DTU, was carried out within the framework of the EFDA. The content of the publication is the sole responsibility of its authors and it does not necessarily represent the views of the Commission or its services. This work was also supported by grant P19901 of the Austrian Science Fund (FWF).

References

[1] C. Ionita, N. Vianello, H.W. Müller, et al., J. Plasma Fusion Res. Series 8, 413 (2009).

[2] B. Nold, G.D. Conway, T. Happel, et al., Plasma Phys. Control. Fusion 52, 065005 (2010).